Supplementary Information

Anomalous orbital structure in a spinel-perovskite interface

Yanwei Cao,[1,*] Xiaoran Liu,[1] P. Shafer,[2] S. Middey,[1] D. Meyers,[1,3] M. Kareev,[1]
Z. Zhong,[4,5] J.-W. Kim,[6] P. J. Ryan,[6] E. Arenholz,[2] and J. Chakhalian[1]

[1]*Department of Physics, University of Arkansas, Fayetteville, AR 72701, USA*
[2]*Advanced Light Source, Lawrence Berkeley National Laboratory, Berkeley, California 94720, USA*
[3]*Department of Condensed Matter Physics and Materials Science, Brookhaven National Laboratory, Upton, NY 11973, USA*
[4]*Institut für Theoretische Physik und Astrophysik, Universität Würzburg, Am Hubland, Germany*
[5]*Max-Planck-Institut für Festkörperforschung, Heisenbergstrasse 1, 70569 Stuttgart, Germany*
[6]*Advanced Photon Source, Argonne National Laboratory, Argonne, Illinois 60439, USA.*

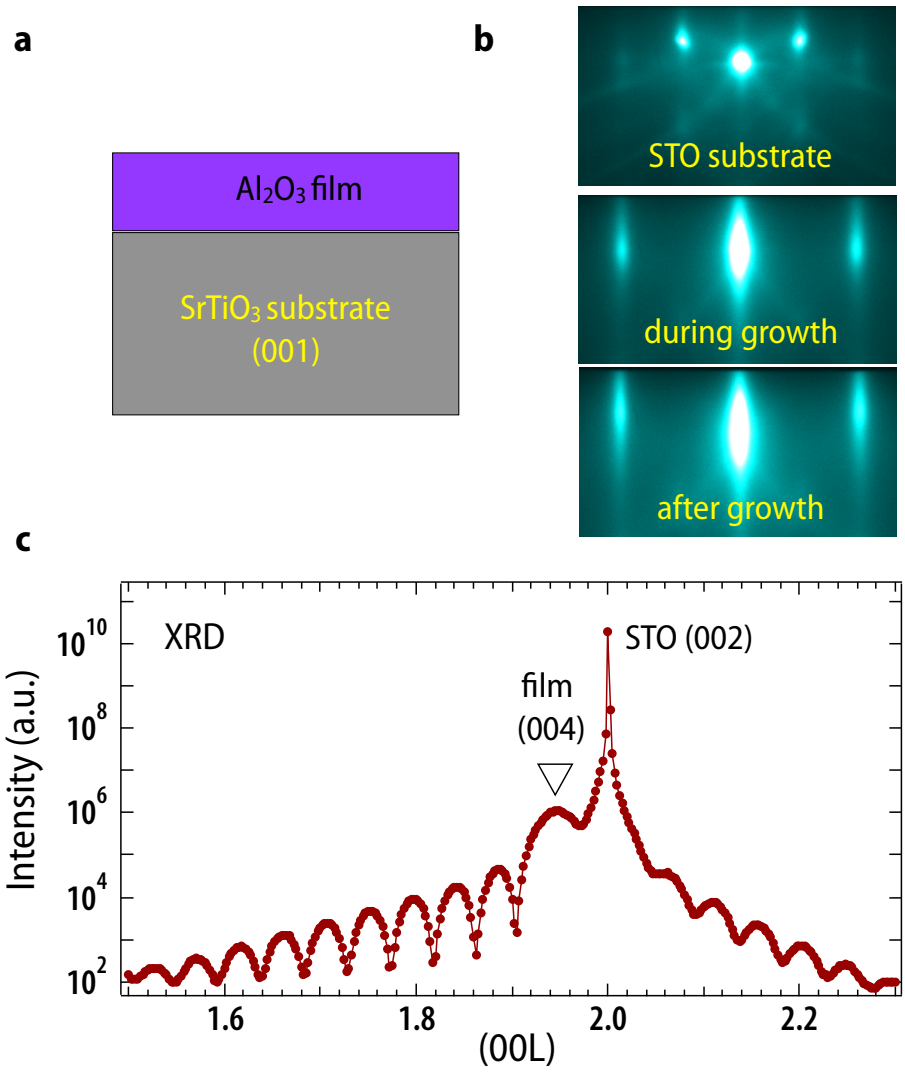

FIG. 1 | **(Supplementary Figure 1) Synthesis and characterization of AlO/STO heterostructures.** (**a**) Schematic view. (**b**) RHEED patterns of $SrTiO_3$ substrate and γ-Al_2O_3 layers during growth. (**c**) XRD data (room temperature) of AlO/STO around (004) peak with distinct thickness fringes. The black triangle indicates the feature associated with the Al_2O_3 film.

* yc003@uark.edu

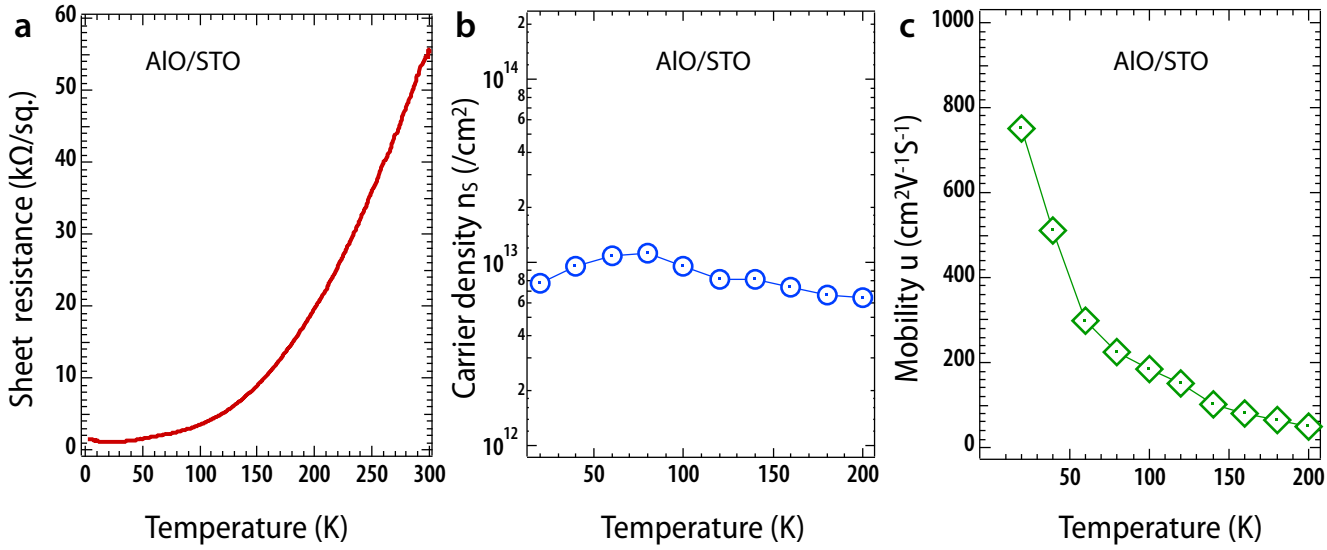

FIG. 2 | **(Supplementary Figure 2) Electrical transport of AlO/STO heterostructure.** (**a**) Sheet resistance. (**b**) Carrier density. (**c**) Carrier mobility.

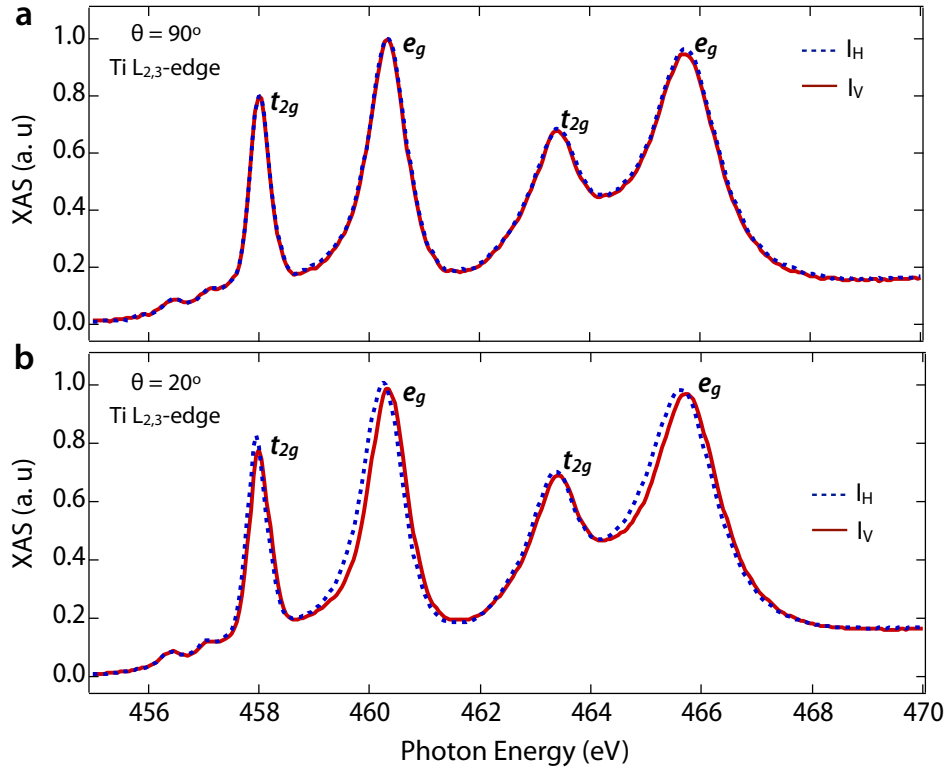

FIG. 3 | **(Supplementary Figure 3) Zoom in of linearly polarized XAS in Fig. 1(b),(c).** (**a**) Incident angle θ = 90°. (**b**) Incident angle θ = 20°. In-plane [I_V, $E_V \parallel ab$ and E is the linear polarization vector of the photon] and out-of-plane [I_H, θ is the angle between E_H and c] linearly polarized X-ray were used to measure XAS of AlO/STO at Ti $L_{2,3}$-edge with total electron yield (TEY, interface sensitive) detenction mode at room temperature.

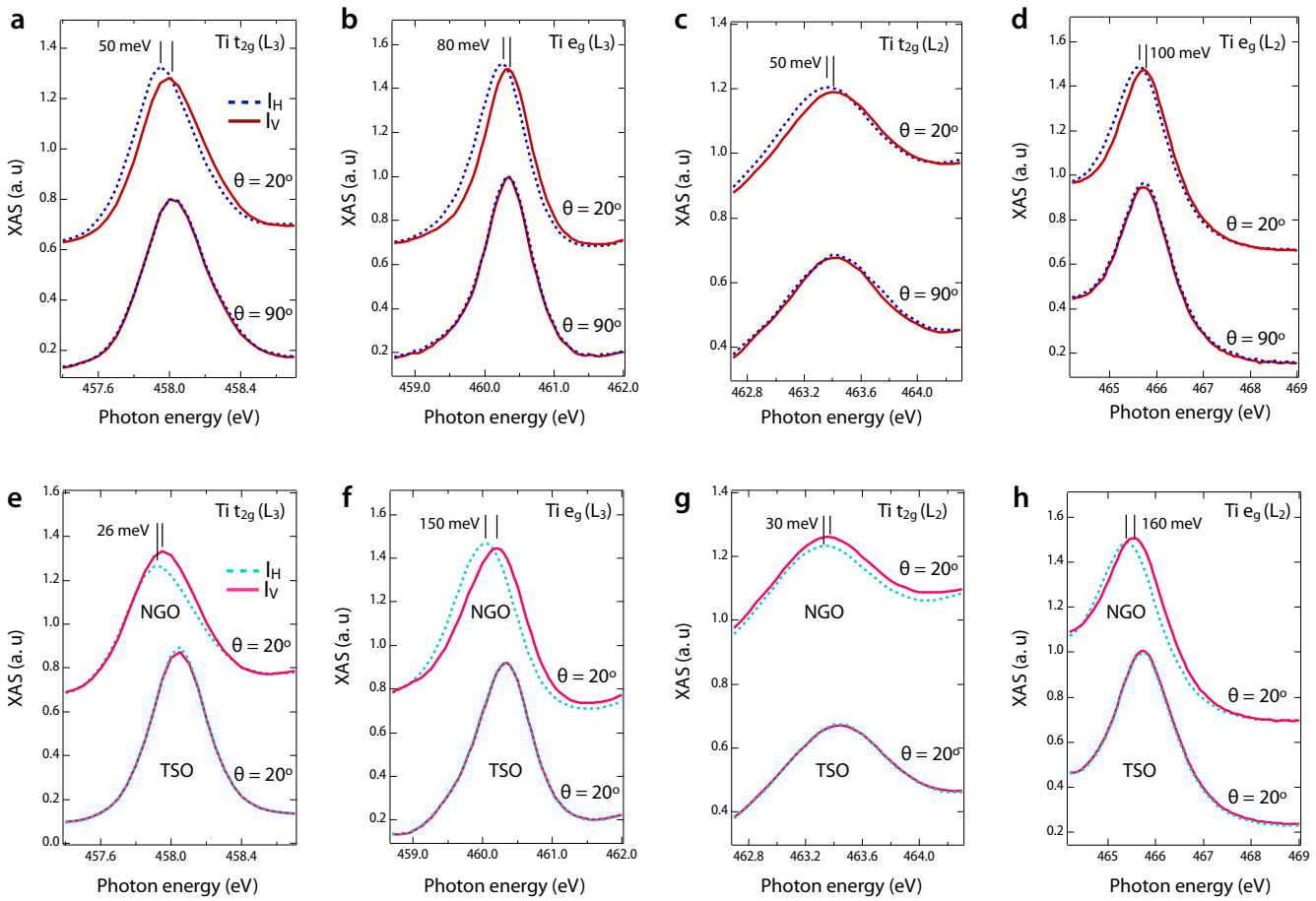

FIG. 4 | **(Supplementary Figure 4) Crystal field splitting of AlO/STO heterostructures.** (**a-d**) Ti t_{2g} and e_g splitting of AlO/STO for an x-ray angle of incidence $\theta = 20^\circ$ and 90°, respectively. (**e-h**) Ti t_{2g} and e_g splitting of AlO/STO for an x-ray angle of incidence $\theta = 20^\circ$ on tensile $TbScO_3$ and compressive $NdGaO_3$ substrates, respectively.

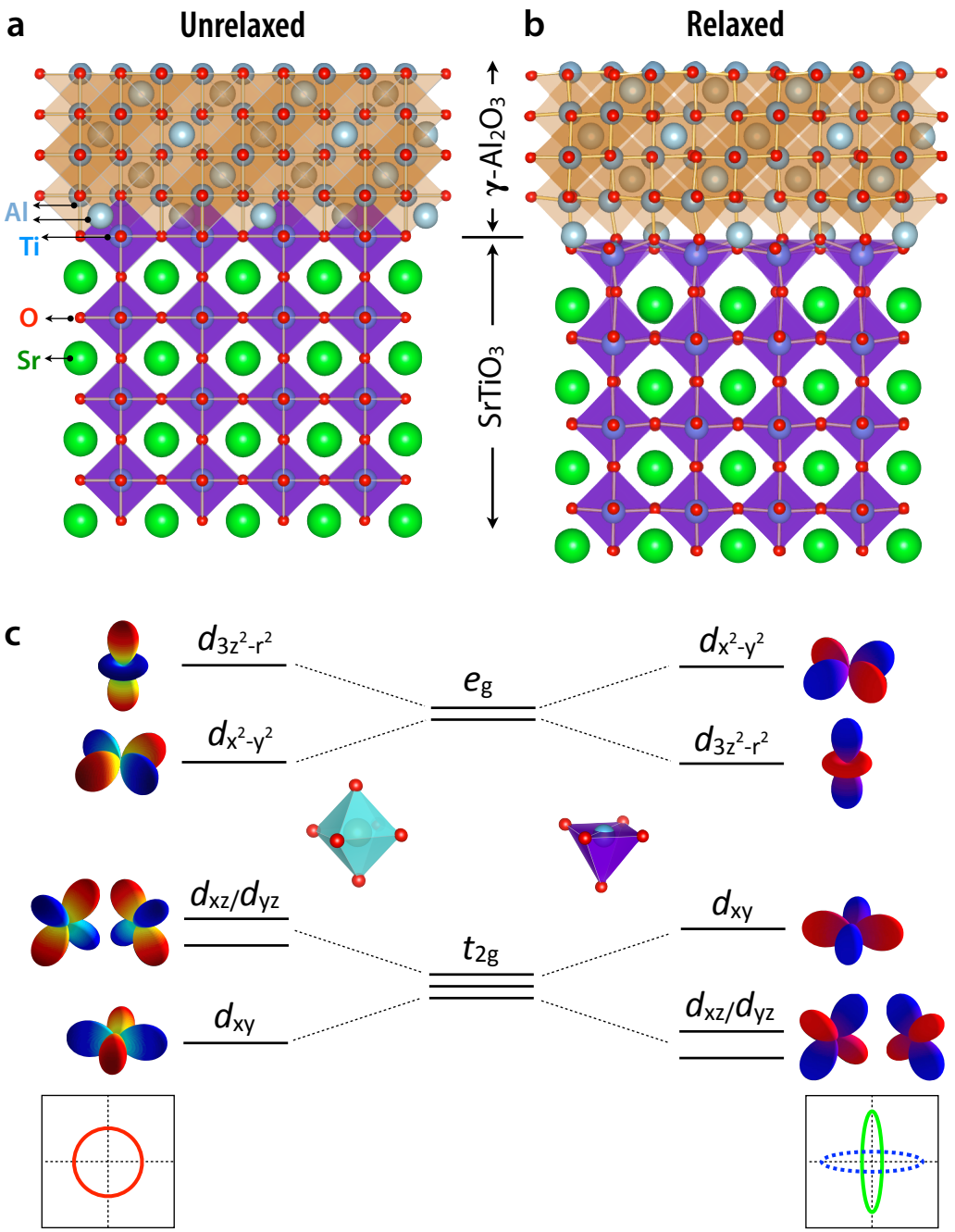

FIG. 5 | **(Supplementary Figure 5) Anisotropic and isotropic Fermi surface map depending on preferential orbital structure.** (**a**),(**b**) Schematic interfacial structures of unrelaxed and relaxed AlO/STO heterostructures, respectively. (**c**) Schematic of Ti $3d$ crystal field splitting in octahedral and pyramidal symmetries. Anisotropic Fermi surface map (blue and green curves) mainly arises from the conduction electrons with d_{xz}/d_{yz} orbitals, whereas isotropic Fermi surface map is mainly contributed by the conduction electrons with d_{xy} orbital character leading to a circle-like isotropic map of Fermi surface (red circle).